



Originally published as:

Marotta, A. M., Bayer, U., Scheck, M., Thybo, H. (2001): The stress field below the NE German Basin: Effects induced by the Alpine Collision. - *Geophysical Journal International*, 144, 2, pp. F8—F12.

DOI: <http://doi.org/10.1046/j.1365-246x.2001.00373.x>

FAST-TRACK PAPER

The stress field below the NE German Basin: effects induced by the Alpine collision

A. M. Marotta,^{1,2} U. Bayer,² M. Scheck² and H. Thybo³

¹ *Università degli Studi di Milano, Department of Earth Sciences, Sec. Geophysics, L. Cicognara, 7 I-20129 Milan, Italy.*

E-mail: anna.maria.marotta@unimi.it

² *GFZ-Potsdam 4.3, Telegrafenberg s/n, D-14473 Potsdam, Germany*

³ *Geological Institute, University of Copenhagen, Oster Voldgade 10, DK-1350 Copenhagen K, Denmark*

Accepted 2000 November 10. Received 2000 November 6; in original form 2000 July 14

SUMMARY

We use a thin-sheet approach for a viscous lithosphere to investigate the effects induced by the Alpine collision on the vertical deformation and regional stress in northern Europe, focusing on the NE German Basin. New seismic studies indicate a flexural-type deep crustal structure under the basin, which may be induced by compressive forces transmitted from the south and related to Alpine tectonics. Finite element techniques are used to solve the vertical deformation and stress field for a viscous European lithosphere with horizontal rheological heterogeneities. Our results support the idea that a relatively strong lithosphere below the northern margin of the German Basin at the transition into the Baltic Shield may explain the characteristic regional stress field, especially the fan-like pattern that is observed within the region.

Key words: Alpine collision, lithosphere, NE German basin, stress.

INTRODUCTION

Several attempts have been made in recent years to model the present-day stress field in the European region caused by plate boundary forces and intraplate compressive stresses (Grünthal & Stromeyer 1986, 1992; Richardson 1992; Gölke & Coblenz 1996). In these studies the modelling results are compared with the World Stress Map by Zoback (1992), which shows a broad-scale NW–SE uniform pattern of the direction of maximum horizontal stress (S_{Hmax}) in the western part of Central Europe, with a rotation toward E–W in the easternmost part of Europe and around the Pannonian Basin (Müller *et al.* 1992). These studies are in general successful in simulating the general pattern of the stress field in western Europe, which is a result of the tectonic forces arising from North Atlantic seafloor spreading and the convergence between the African and Eurasian plates, but they fail to reproduce the stress pattern in the North German Basin and the eastern intra-Carpathians regions.

A new set of borehole stress data is available in the region of the NE German Basin (Gröte 1998; Roth *et al.* 1997, 1999). While the supra-salt data show a NW–SE to W–E orientation of S_{Hmax} , the orientation is different below the Zechstein salt, where the orientation of S_{Hmax} is N–S to NE–SW, in agreement with the regional World Stress Map. Discarding the stress data from layers above the Zechstein salt, which may be consequences

of local salt movements, the subsalt *in situ* stress data show a fan-like structure in the northern part of the German Basin with a rotation from a westerly to an easterly direction from west to east (Fig. 1a).

A 2-D flexural model (Bayer *et al.* 1999; Marotta *et al.* 1999, 2000) may explain the stress along the seismic profile BASIN-96 (Fig. 1a), which crosses the NE German Basin from the Hartz mountains to the island of Rügen (DEKORP BASIN Research Group 1999). This model supports the idea that localized compressive forces played a dominant role in shaping the deep crustal structure below the NE German Basin. The stresses also played a significant role in the uplift of the Hartz mountains and the corresponding flexural bulge of the lithosphere (Bayer *et al.* 1999; DEKORP BASIN Research Group 1999). In this study we investigate the effects of the compressive forces arising from the Alpine collision on the local stress field in northern Germany, taking into account horizontal heterogeneities in the strength of the lithosphere below the North German Basin.

In the present analysis we use the viscous thin-sheet model of England & McKenzie (1982, 1983). The lithosphere is modelled as a thin plate of variable crustal thickness and constant lithospheric thickness over a non-viscous asthenospheric half-space. The base of the lithosphere is consequently stress-free and the lithosphere is isostatically compensated. In order to solve the deformation and the stress field, the equations for the horizontal deformation and for the time variation of the crustal

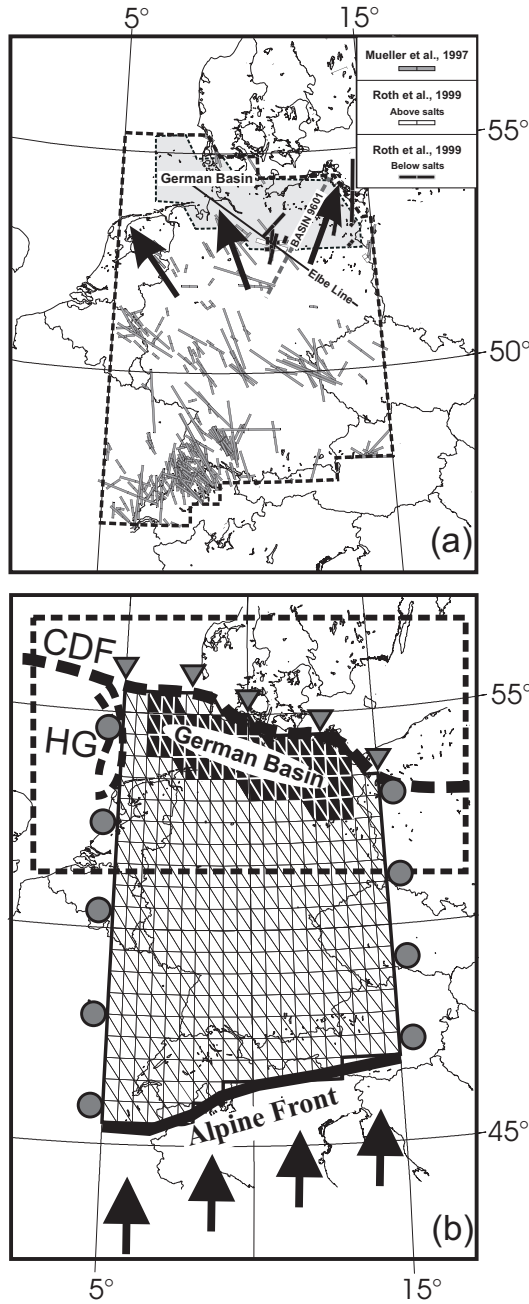


Figure 1. (a) World Stress Map (Mueller *et al.* 1997) updated with results from Roth *et al.* (1997, 1999). The bold dashed line delimits the region under study. The Elbe line and seismic section BASIN 9601 are also shown. Large arrows indicate the averaged direction of the compressive stress in N Germany. (b) Finite element mesh for the entire area under study with the assumed boundary conditions given in terms of velocity, stress and crustal thickness. On the upper boundary (the Caledonian Deformation Front) we applied no-slip conditions (triangles), i.e. both components of velocity equal to zero. At the lower boundary (Alpine front) we fixed the velocity (large arrows) at 0.4 cm yr^{-1} towards the north (Bonini *et al.* 1999; Schmid *et al.* 1996, 1997). At the lateral boundaries we assumed zero shear stress (circles). As a second condition, two different models have been tested, one with closed lateral sides (horizontal component of velocity equal to zero) and one with open lateral sides and zero horizontal gradient of the horizontal velocity component. We kept the crustal thickness fixed at all of the sides of the modelled region. CDF: Caledonian Deformation Front; HG: Horn Graben. The dashed bold line delimits the area that we refer to in Figs 2, 3 and 4.

thickness s ,

$$\frac{\partial}{\partial x_j} \left[I \dot{E}^{(n-1)} \dot{\epsilon}_{ij} \right] - \frac{\partial}{\partial x_i} \left[I \dot{E}^{(n-1)} \dot{\epsilon}_{zz} \right] = \frac{1}{2} \text{Ar} \frac{\partial s^2}{\partial x_i} \quad (i, j = 1, 2), \quad (1)$$

$$\frac{\partial s}{\partial t} = - \frac{\partial}{\partial x_1} (s u_1) - \frac{\partial}{\partial x_2} (s u_2), \quad (2)$$

are solved numerically by a newly developed finite element code. $\dot{E} = (\dot{\epsilon}_{ij} \dot{\epsilon}_{ij})^{1/2}$ is the second invariant of the strain rate $\dot{\epsilon}_{ij}$. Ar is the Argand number, defined as

$$\text{Ar} = \frac{g \rho_c L (1 - \rho_c / \rho_m)}{B_o (u_o / L)^{1/n}}. \quad (3)$$

This parameter is a measure of the relative importance of the viscous and buoyancy forces and is a constant for the whole modelled area once the values for the reference rheological coefficient, B_o (the depth-averaged strength coefficient, corresponding to a reference effective viscosity of $10^{21}/10^{22}/10^{23}$ Pa s), as well as u_o (the reference velocity— 0.4 cm yr^{-1}), L (the lithosphere thickness—100 km), ρ_c and ρ_m (the crustal and mantle densities—2800 and 3300 kg m^{-3} respectively) are specified. $I = B/B_o$ is the rigidity ratio between the modelled inclusion and the surrounding area. We use a linear creep law to express the rheological behaviour of the system. A set of triangular elements (with three nodes and seven Gaussian points for the numerical integration) covers the modelled region with a spatial resolution of about 0.5° (Fig. 1b). We did not include any internal faults in the model. The presence of the German Basin is simulated by introducing horizontal heterogeneity in the effective viscosity of the lithosphere. Thus, different numerical experiments were carried out with local ratios B/B_o of 0.1, 1, 20 and 100 for all the elements used to fit the German Basin and different boundary conditions in terms of velocity and crustal thickness. Since we focus our analysis on the new compilation of stresses in the N German basin (Roth *et al.* 1997, 1999), we show the results for a model that extends from the Alpine front to the Caledonian Deformation Front, and from the Horn Graben to about 15°E . Table 1 shows the numerical values of the parameters used in the numerical calculations.

We consider only the last 32 Myr of convergence, the time interval corresponding to the Alpine collisional and post-collisional phases, during which we assume that the Adriatic plate acted for all the length of the Alpine front as a rigid indenter, responsible for the thickening of the European crustal margin. Although this assumption is strictly correct only where the Ivrea body is present (Schmid & Kissling, 2000), the use of a rigid indenter in order to approximate the advancing Alpine front rather than a deformable front is not a crucial limit since

Table 1. Values of the parameters used in the numerical calculations.

Parameter	Description	Value
L	Lithosphere thickness	100 km
ρ_c	Density of crust	2800 kg m^{-3}
ρ_m	Density of mantle	3300 kg m^{-3}
G	Gravitational acceleration	9.8 m^{-2}
u_o	Reference velocity	0.4 cm s^{-1}
$\mu_o \text{ eff}$	Reference effective viscosity	$10^{21}/10^{22}/10^{23} \text{ Pa s}$

our analysis does not consider the Alpine deformation as part of the study. We use an advancement velocity of 0.4 cm yr^{-1} (Bonini *et al.* 1999; Schmid *et al.* 1996, 1997) and a time step of 0.1 Myr in order to keep the maximum deformation of each element below 5 per cent of the initial dimension. In order to define the position of the front at the starting time, we retreat the southern front about 128 km to the south with respect to the present-day position. As an initial condition for the crustal thickness, we implement two different cases. In the first we assume an initial homogeneous crustal thickness of 35 km. This value is representative of the present-day horizontally averaged value of crustal thickness as documented by Blundell *et al.* (1992) and Thybo (2000). However, since the displacement of the Alpine front during the last 32 Myr was small in comparison with the total horizontal length of the studied region, we expect that it might have had a stronger effect on the stress field than on the deformation field. Thus we implemented other cases that use the present-day crustal thickness as the initial condition. The results shown in Figs 2, 3 and 4 refer to the latter case.

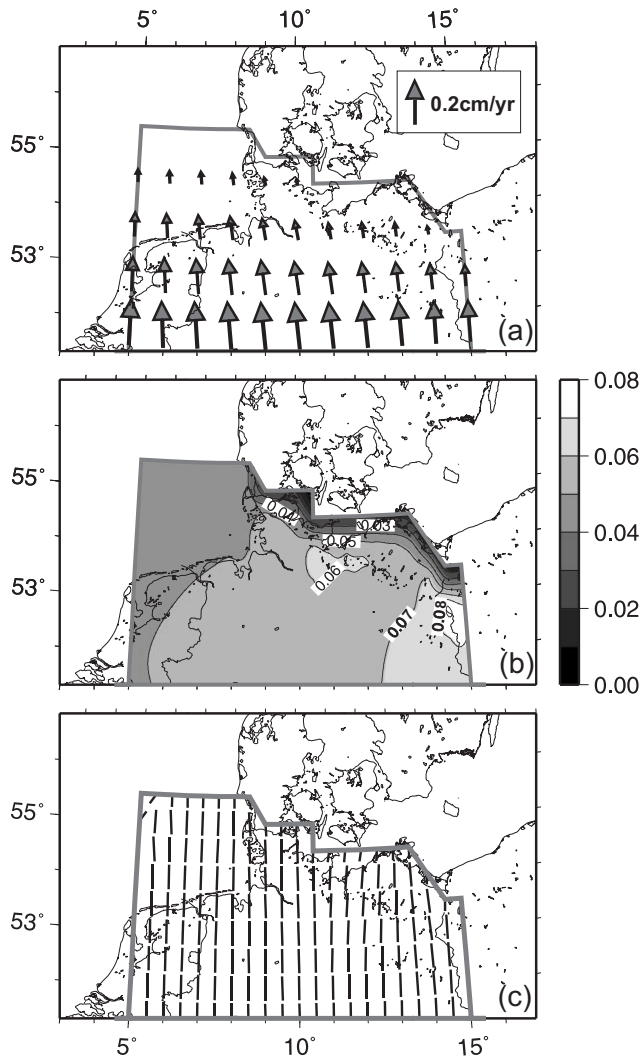


Figure 2. (a) Velocity field, (b) normalized strain rate and (c) S_{Hmax} direction in the N German basin for a viscous lithosphere, with no horizontal rheological heterogeneities.

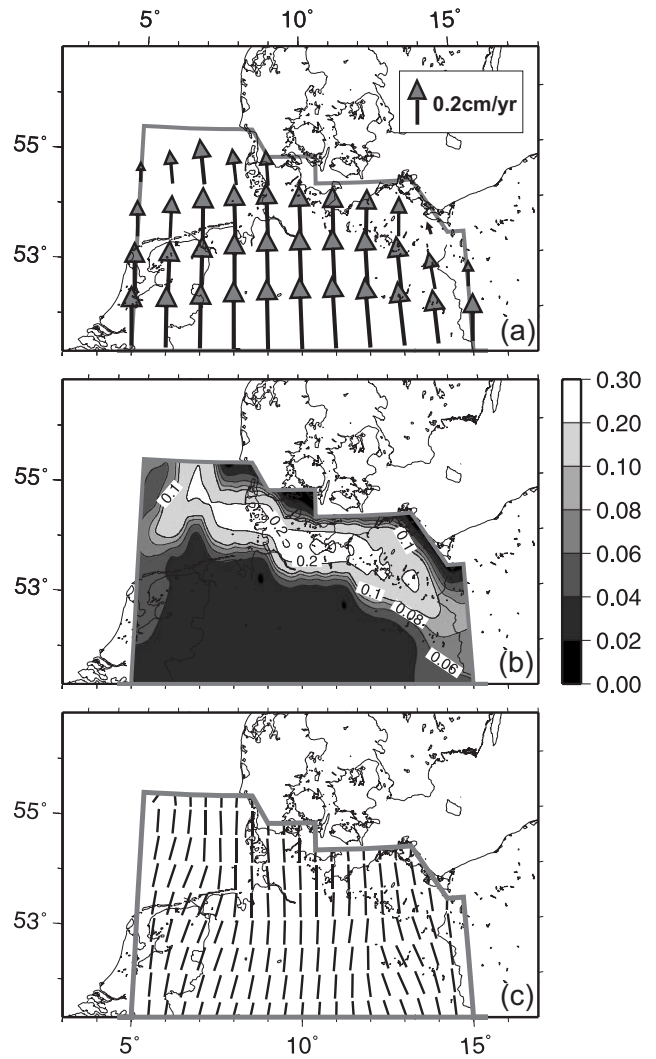


Figure 3. (a) Velocity field, (b) normalized strain rate and (c) S_{Hmax} direction in the N German Basin for a locally weak lithosphere model. The results refer to a ratio of $B/B_0 = 0.1$ assumed in all the elements of the N German Basin.

RESULTS

We developed a series of models that differ with regard to the boundary conditions, the Argand number and the local average rheology. For all of the models the shape of the analysed region does not affect significantly the distribution of the stress field.

In the case of a homogeneous lithosphere, the velocity field shows an almost homogeneous pattern (Fig. 2a), with the velocity vectors generally aligned as a continuation of the velocity of the southern boundary. Only at the northeastern border does the velocity field show small deviations due to the irregular shape of the boundary of the modelled region. Consequently, the vertical strain rate increases only in the W–E direction, while it is relatively constant in the N–S direction, coherently with the velocity field pattern (Fig. 2b). The stress field shows a broad-scale uniformity with a general S–N direction, which is consistent with the tectonic forces arising from the S–N convergence (Fig. 2c) and in agreement with previous modelling studies (Grünthal & Stromeyer 1986, 1992).

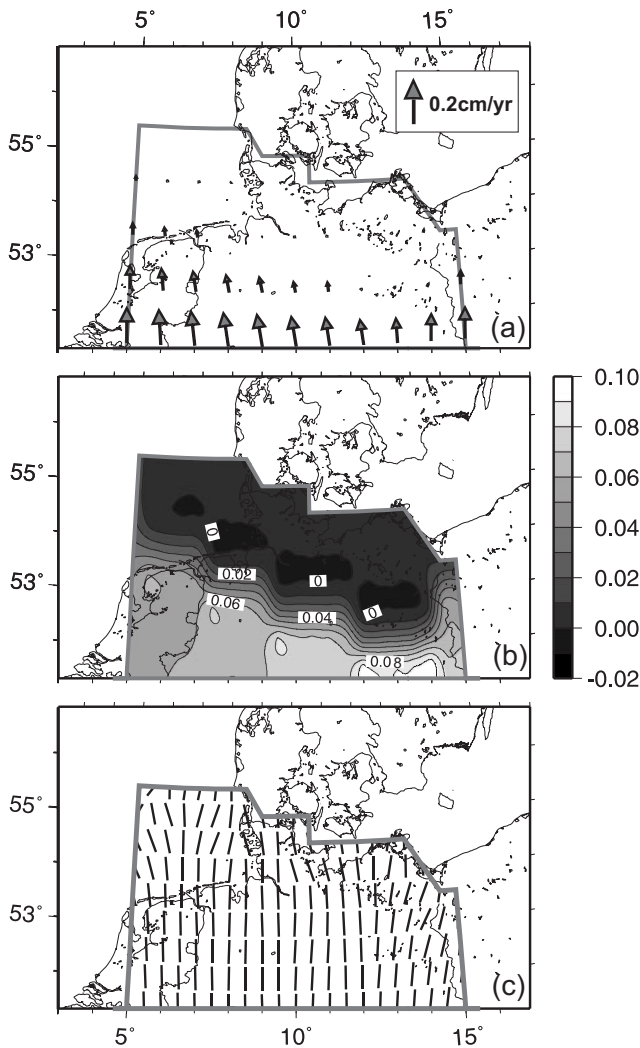


Figure 4. (a) Velocity field, (b) normalized strain rate and (c) S_{Hmax} direction in the N German Basin for a locally viscous strong lithosphere model. The results refer to a ratio of $B/B_0=100$ assumed in all the elements of the N German Basin.

If we introduce horizontal heterogeneity in order to simulate the N German Basin, the general strain and stress pattern changes significantly. Two different cases have been studied. In the first case we assume a reduced strength of the lithosphere below the basin, as would result from a thick sedimentary layer or from local heating. In the second case we assume a stronger lithosphere below the German Basin. A detailed rheological study of the area (Marotta *et al.* 1999, 2000) supports the idea that the German Basin is stronger than the surrounding regions. This increase in the local strength is also consistent with other geophysical parameters: high lower crustal seismic velocities (Thybo 1990; Rabbel *et al.* 1995; Bleibinhaus *et al.* 1999) and high lower crustal density, as indicated by gravity modelling (Scheck *et al.* 1999; Bayer *et al.* 1999).

The main effect of introducing a weak lithosphere is that the stiffer European lithosphere moves almost with a constant velocity toward the north and all the strain is concentrated within the weak N German lithospheric block, which undergoes progressive local thickening (Figs 3a and b). Considering

the distribution of the principal horizontal stress distribution, we find a general rotation of S_{Hmax} towards the centre of the basin (Fig. 3c), in the opposite direction to the observed stress pattern (Fig. 1a).

When a strong lithosphere is considered below the N German Basin, the region below the basin remains mainly undeformed and the basin acts as a 'barrier' for the transmission of stress (Fig. 4). Consequently, the direction of S_{Hmax} undergoes a local rotation towards the external part of the basin (Fig. 4c). These results are in agreement with the mean compressive stress direction based on the World Stress Map (Mueller *et al.* 1997) and the new borehole data (Roth *et al.* 1997, 1999), as summarized in Fig. 1a. We have verified that this remarkable result is independent of the boundary conditions and small changes of the Argand number. The deviation in the direction of S_{Hmax} in our model in the central part of the studied region from the observed direction could be related to the Elbe line system of faults (Fig. 1a), situated north of the region where this deviation is observed. This system of faults, not yet included in our model, could be responsible for the local westward rotation in the direction of S_{Hmax} .

CONCLUSIONS

Our modelling results show the effects of the late Cretaceous–early Tertiary Alpine compression on the stress field below the N German Basin. The analysis of the velocity and strain fields and of S_{Hmax} directions leads to the following conclusions.

(1) The observed local stress pattern below the N German Basin can be reproduced with reasonable agreement by a 2-D thin-sheet finite element model that takes into account the last 32 Myr of post-collisional Alpine convergence and assumes a rheological anomaly for the lithosphere below the N German Basin. Our study shows that the general broad-scale NW–SE S_{Hmax} direction in the western part of Europe originated basically from the tectonic forces induced by Alpine compression, in agreement with previous models. In the N German Basin, the fan-like stress pattern, with deviations in the S_{Hmax} direction from NW–SE in the western region to NE–SW in the eastern region, can be explained by assuming a stronger lithosphere below the basin, which therefore acts as a local barrier to the transmission of tectonic forces.

(2) With regards to the recent observations in connection with the deep seismic survey BASIN-96 (DEKORP BASIN Research Group 1999; Bayer *et al.* 1999), we conclude that the N German Basin is still in a state of horizontal compression and therefore not in isostatic equilibrium. This aspect has previously been considered in a gravity study (Scheck *et al.* 1999).

ACKNOWLEDGMENTS

This work was supported by the EU-founded network PACE (Palaeozoic Amalgamation of Central Europe). We are grateful to our PACE colleagues for the fruitful discussions at PACE and EUROPROBE workshops, especially within the TESZ project. We thank Frank Roth for allowing us to use the new stress data in the NE German Basin. Valuable discussions with Roberto Sabadini are greatly appreciated. All illustrations were made using the Generic Mapping Tools (GMT) of Wessel & Smith (1998).

REFERENCES

- Bayer, U. *et al.*, 1999. An integrated study of the NE German Basin, *Tectonophysics*, **314**, 285–307.
- Bleibinhaus, F., Beilecke, T., Braum, K. & Gebrande, H., 1999. A seismic velocity model for the SW Baltic Sea derived from BASIN'96 refraction seismic data, *Tectonophysics*, **314**, 269–283.
- Blundell, D., Freeman, R. and Müller, St., eds, 1992. *A Continent Revealed: the European Geotraverse*, Cambridge University Press, Cambridge.
- Bonini, M., Sokoutis, D., Talbot, C.J., Boccaletti, M. & Milnes, A.G., 1999. Indenter growth in analogue models of Alpine-type deformation, *Tectonics*, **18**, 119–128.
- DEKORP BASIN Research Group, 1999. The deep structure of the NE German Basin—constraints on the controlling mechanisms of intracontinental basin development, *Geology*, **27**, 55–58.
- England, P. & McKenzie, D., 1982. A thin viscous sheet model for continental deformation, *Geophys. J. R. astr. Soc.*, **70**, 295–321.
- England, P. & McKenzie, D., 1983. Correction to: a thin viscous sheet model for continental deformation, *Geophys. J. R. astr. Soc.*, **73**, 523–532.
- Gölke, M. & Coblenz, D., 1996. Origin of the European regional stress field, *Tectonophysics*, **266**, 11–24.
- Gröte, R., 1998. Die rezente horizontale Hauptspannungsrichtung im Totliegenden und Oberkarbon in Norddeutschland, *Geologie*, **114**, 478–483.
- Grünthal, G. & Stromeyer, D., 1986. Stress pattern in Central Europe and adjacent areas, *Gerlands Beitr. Geophys.*, **95**, 443–452.
- Grünthal, G. & Stromeyer, D., 1992. The recent crustal stress field in Central Europe: trajectories and finite element modeling, *J. geophys. Res.*, **97**(B8), 11 805–11 820.
- Marotta, A.M., Bayer, U. & Thybo, H., 1999. A 2-D flexural model for crustal deformation below the NE German Basin, *EUG10, Strasbourg* (abstract vol.).
- Marotta, A.M., Bayer, U. & Thybo, H., 2000. The legacy of the NE-German Basin—reactivation by compressional buckling, *Terra Nova*, in press.
- Müller, B., Zoback, M.L., Fuchs, K., Mastin, L., Gregensen, S., Pavoni, N., Stephansson, O. & Ljunggren, C., 1992. Regional pattern of tectonic stress in Europe, *J. geophys. Res.*, **97**, 11 783–11 803.
- Mueller, B., Wehrle, V. & Fuchs, K., 1997. *The 1997 release of the World Stress Map*, <http://www-wsm.physik.uni-karlsruhe.de/pub/Rel97/wsm97.html>.
- Rabbel, W., Föste, K., Schulze, A., Bitter, R., Röhl, J. & Reichert, J.C., 1995. A high-velocity layer in the lower crust of the North German Basin, *Terra Nova*, **7**, 327–337.
- Richardson, R.M., 1992. Ridge forces, absolute plate motions and the intraplate stress field, *J. geophys. Res.*, **97**, 11 739–11 748.
- Roth, F., Sperner, B., Jarosinski, M., Krupsky, Y., Weigold, G., Bäbler, H. & Müller, B., 1997. Orientation of tectonic stress from boreholes in NE Germany, Poland and the Western Ukraine, *Terra Nostra*, **11**, 118–120.
- Roth, F., Fleckenstein, P., Palmer, J. & Groß, U., 1999. Stress orientations found in NE Germany differ from the West European trend, *Proc. ICDP/KTB Kolloquium, Bochum*, 255–264.
- Scheck, M., Barrio-Alvers, L., Bayer, U. & Götze, H.J., 1999. Density structure of the Northeast German Basin; 3D modelling along the DEKORP Line BASIN96, *Phys. Chem. Earth*, **A21**, 221–230.
- Schmid, S.M. & Kissling, E., 2000. The arc of the western Alps in the light of geophysical data on deep crustal structure, *Tectonics*, **19**, 62–85.
- Schmid, S.M., Pfiffner, O.A., Froitzheim, N., Schönborn, G. & Kissling, E., 1996. Geophysical-geological transect and tectonic evolution of the Swiss-Italian Alps, *Tectonics*, **15**, 1036–1064.
- Schmid, S.M., Pfiffner, O.A., Schönborn, G., Froitzheim, N. & Kissling, E., 1997. Integrated cross section and tectonic evolution of the Alps along the Eastern Traverse, in *Deep Structure of the Swiss Alps: Results of NRP 20*, pp. 289–304, eds Pfiffner, O.A., Lehner, P., Heitzmann, P., Muller S. & Stek, A., Birkhäuser, Boston, MA.
- Thybo, H., 1990. A seismic velocity model along the EGT profile—from the North German Basin into the Baltic shield, in *The European Geotraverse. Integrative Studies*, pp. 99–108, eds Freeman, R., Giese, P. & Müller, St., European Science Foundation, Strasbourg.
- Thybo, H., 2000. Crustal structure and tectonic evolution of the Tornquist Fan region as revealed by geophysical methods, *Bull. geol. Soc. Denmark*, **46**, 145–160.
- Wessel, P. & Smith, W.M.F., 1998. New, improved version of generic mapping tools released, *EOS, Trans. Am. geophys. Un.*, **79**, 579.
- Zoback, M., 1992. First- and second-order patterns of stress in the lithosphere: the World Stress Map project, *J. geophys. Res.*, **97**, 11703–11728.